Retrieving the Root-Zone Soil Moisture from Surface Soil Moisture or Temperature Estimates: A Feasibility Study Based on Field Measurements

J.-C. CALVET, J. NOILHAN, AND P. BESSEMOULIN

Météo-France/CNRM, Toulouse, France

(Manuscript received 19 March 1997, in final form 31 July 1997)

ABSTRACT

The bulk soil water content must be estimated accurately for short- and medium-term meteorological modeling. A method is proposed to retrieve the total soil moisture content as well as the field capacity from observed surface parameters such as surface soil moisture or surface temperature. A continuous series of micrometeorological and soil water content measurements was obtained in southwestern France over a fallow site in 1995. In addition, the database includes measurements of the surface temperature and soil moisture profiles within the top 5-cm soil layer. The surface soil moisture measurements are available twice a day during two 30-day intensive observing periods in spring and autumn 1995. Once calibrated, the ISBA (Interactions between Soil, Biosphere, and Atmosphere) surface scheme is able to properly simulate the measured surface variables and the bulk soil moisture. Then an assimilation technique is applied to analyze the field capacity and the total soil water content from the surface data. In particular, it is shown that knowing the atmospheric forcing and the precipitation, four or five estimations of the surface soil moisture spread out over a 15-day period are enough to retrieve the total soil water content by inverting ISBA. The use of the surface temperature seems more problematic because its sensitivity to the value of the total water content is meaningful in relatively dry conditions only.

1. Introduction

The estimation of the soil water content in the root zone is an important issue for short-term meteorological modeling. The surface schemes now employed in meteorology are designed to describe the basic evaporation processes at the surface together with the water partitioning between the vegetation transpiration, the drainage, the surface runoff, and the soil moisture increase or decrease. For example, the ISBA (Interactions between Soil, Biosphere, and Atmosphere) scheme (Noilhan and Planton 1989) is used in the operational simulations of the French weather forecast model ARPEGE (Action de Recherche Petite Echelle–Grande Echelle). One of the main difficulties in the use of such parameterizations is the initialization of the soil wetness.

In recent years, attempts were made to retrieve the root-zone soil moisture from screen-level variables (air temperature and humidity) by inverting simple surface schemes [e.g., Mahfouf (1991), with the ISBA scheme]. In some conditions, it is possible to adjust the value of the root-zone soil water content in order to minimize the forecast error on the low-level atmospheric parameters. A difficulty of this method is that the link between screen-level parameters and the root-zone soil water content is rather indirect. An alternative method consists in using remote sensing thermal infrared or microwave techniques to obtain surface variables such as surface temperature or surface soil moisture. The surface variables may be more easily related to the soil water content than screen-level parameters (air temperature and humidity) over large areas because they directly reflect the surface energy balance. Several authors (e.g., Wetzel et al. 1984; McNider et al. 1994; van den Hurk et al. 1997) have proposed assimilation techniques based on data from meteorological satellites. Wetzel et al. (1984) show that, in relatively dry conditions, the diurnal change in surface skin temperature as estimated from satellite data can be employed to retrieve the bulk soil water content.

Other remote sensing techniques, such as active or passive microwaves, are likely to provide information about the moisture of a shallow surface soil layer—5 cm or less (Schmugge 1983). The surface soil moisture can be retrieved over vegetated surfaces since vegetation canopies generally do not totally screen the soil microwave emission at low frequencies (L band). To a lesser extent, passive microwaves also provide information about surface temperature (e.g., Calvet et al. 1996). The use of passive microwaves for soil moisture retrieval was investigated theoretically by Entekhabi et al. (1995) in the case of a bare soil. They showed that it is possible to retrieve the soil water content using passive microwave data (at frequencies less than 10 GHz). In their study,

Corresponding author address: Dr. Jean-Christophe Calvet, Météo-France/CNRM/GMME/MC2, 42, avenue G. Coriolis, 31057 Toulouse Cedex 1, France.
E-mail: calvet@meteo.fr

the propagation of the information from the deepest layers to the soil surface is investigated using a complex multilayer model of the heat and water transfers for a bare soil.

A first step before using the microwave radiometry technique consists of testing the feasibility of using an operational scheme like ISBA to retrieve the root-zone soil water content from in situ measurements of the surface soil moisture, in the case of a vegetated surface. The central question addressed in this paper is how to put the ISBA physics to best use in order to estimate the root-zone soil moisture from time series observations of the surface soil moisture. In this study, the ISBA model is run for the highly instrumented field site of the MUREX (Monitoring the Usable Soil Reservoir Experimentally) experiment (Bessemoulin et al. 1996), over which long-term weekly measurements of the root-zone soil moisture and direct measurements of the soil moisture at the surface (during two 30-day intensive observing periods in spring and autumn 1995) are available. Also, the surface temperature derived from infrared and direct measurements at the soil surface is considered. First, it is shown that ISBA, once calibrated, is able to simulate the bulk soil water content over the full annual cycle. Second, the simulated surface soil moisture is compared with the measurements and a sensitivity analysis demonstrates the close dependence of the modeled surface soil moisture upon the initial root-zone soil moisture. Finally, an assimilation technique is applied to analyze the field capacity and the bulk soil water content from the surface data (either surface soil moisture or surface temperature).

2. Data and site characteristics

The micrometeorological station of the MUREX experimental site (43°24′N, 1°10′E; altitude 240 m) was set up in June 1994. In this study, data from 1995 are considered. The vegetation canopy of the MUREX site consists of a dense close herbaceous agricultural fallow. The main plant species are *Brachypodium ramosum, Potentilla reptans, Geranium rotundifolium, Erigeron canadensis,* and *Rumex acetosa,* as observed on day of year (DoY) 293 of 1995. The soil is a typical hydromorphic deep ''boulbène'': the mean texture of the 1-m surface soil layer is that of a silt loam (the sand and clay proportions are 14% and 28%, respectively). However, strong vertical gradients of texture are observed: the proportion of clay increases from 17% at the surface to 40% at 1-m depth. On this type of soil, at about 1 m, a local subsurface soil water convergence may sometimes occur, caused by a temporary perched water table over the clay bedrock.

The meteorological variables (precipitation, air temperature and humidity, and wind speed and direction) at the site were monitored on a 30-min basis together with surface temperature, solar radiation, and the surface fluxes: net radiation Rn, sensible heat flux H, ground heat flux G, and by difference the latent heat flux LE = Rn − H − G. The other routine surface measurements consist of weekly profiles of the deep soil moisture content and a characterization of the vegetation.

a. Routine soil and atmospheric data

The soil and atmospheric measurements of MUREX were obtained using methods very similar to those of HAPEX–MOBILHY (Hydrological Atmospheric Pilot Experiment–Modélisation du Bilan Hydrique) (André et al. 1986): classic meteorological observations are combined with surface energy and water budget measurements.

1) ATMOSPHERIC MEASUREMENTS

The equipment employed is similar to the Système Automatique de Mesure se l'Evapotranspiration Réelle station described in Goutorbe (1991). Air temperature and humidity are measured at screen level (2 m). The wind speed U and direction are measured by a propeller anemometer at 10 m above the soil surface. The atmospheric pressure is measured and recorded automatically. The station is also able to document the surface energy balance: the net radiation is measured together with the ground heat flux, and the sensible heat is calculated from two-level measurements (1.5 m apart) of air temperature and wind speed. The accuracy of the two-level measurements (air temperature and wind speed vertical gradients) is one order of magnitude better than the original design: the sensors have been changed and thoroughly intercompared at the same level, under very distinct atmospheric conditions (i.e., different diurnal cycles, strong and low winds, rain/no rain, etc.). The sensor accuracy is now 0.02 m s^{-1} and 0.01°C for wind speed and air temperature, respectively, compared to 0.1 m s^{-1} and 0.1°C for the original sensors.

Rainfall P is recorded automatically from a tipping bucket rain gauge. Also, shortwave and total (0.3–60 μm), upward, and downward radiations are measured. The MUREX station was very reliable during 1995: less than 6% of the surface flux data are missing, 1%–3% of the radiation (the solar incident radiation Rg and the downwelling atmospheric thermal emission Ra), pressure, and air temperature and humidity are missing, and less than 1% of wind speed and precipitation data are missing. To obtain a continuous atmospheric forcing series for 1995, data from neighboring automatic weather stations (Poucharramet, 43°25′N, 1°11′E; altitude 204 m. Ondes, 43°47′N, 1°19′E; altitude 108 m) and of the Francazal airport station (43°32′N, 1°22′E; altitude 164 m) were added to the database. Since the downwelling atmospheric thermal emission Ra is not measured in the supplementary weather stations, the 3% missing data in the original dataset were completed by the following formulation, adapted from Staley and Jurica (1972):

$$\mathrm{Ra} = \beta + \beta'[\sigma_c + (1 - \sigma_c)0.67(1670q_a)^{0.08}]\sigma T_a^4, \quad (1)$$

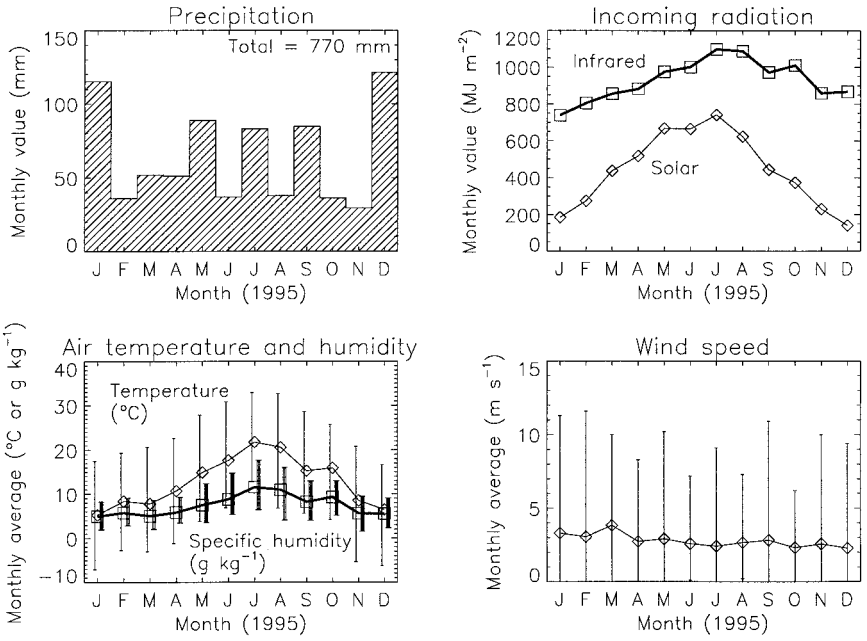

FIG. 1. The measured forcing data of the ISBA scheme (precipitation, P; incoming radiation, Rg and Ra; air temperature and humidity, T_a and q_a; and wind speed, U) over the MUREX fallow in 1995. The plotted precipitation and incoming radiation are monthly sums of the 30-min measured values. Air temperatures, humidity, and wind speed are displayed as monthly means with maximum and minimum values indicated with bars. Air temperature and humidity are represented by diamonds with solid lines and by squares with solid thick lines, respectively.

where σ is the Stefan–Boltzmann constant; T_a and q_a are the air temperature and specific humidity, respectively, at screen level; and σ_c is the cloud coverage ($\sigma_c \in [0, 1]$). The σ_c parameter is measured at Francazal. The regression coefficients β and β' were determined from the 1995 available values of Ra at the MUREX site and of the cloud coverage σ_c at Francazal. The regression parameters are the coefficients $\beta = 11.3$ W m^{-2} and $\beta' = 0.9685$, with a square correlation coefficient r^2 of 73% and a standard error of 25 W m^{-2}. When cloud coverage observations were not available, Eq. (1) was applied with $\sigma_c = 0$, $\beta = 43.9$ W m^{-2}, and $\beta' = 1.0056$. In this case, the value of r^2 is 70% and the standard error is 25 W m^{-2}. Figures 1 and 2 summarize the 1995 measurements of the atmospheric forcing data (Rg, Ra, T_a, q_a, U, P) and of the surface fluxes (Rn, H, LE, G), respectively.

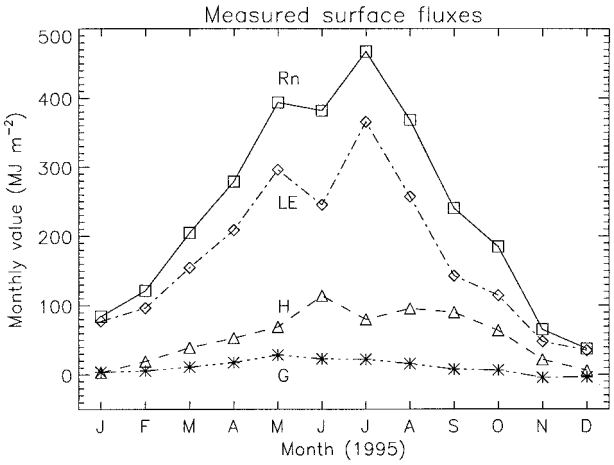

FIG. 2. Monthly sums of the measured fluxes (net radiation, Rn; heat flux, H; latent heat flux, LE; and ground heat flux, G) over the MUREX fallow in 1995. Note that LE is estimated by difference.

2) SOIL MOISTURE MEASUREMENTS

Deep soil moisture profiles are obtained on a weekly basis from neutron probe measurements. The measured soil moisture profiles correspond to regular 0.1-m intervals from the surface to 1.3 m. The soil water potential is estimated from tensiometric measurements at 0.1-m intervals within the 0.3-m surface layer and at 0.2-m intervals below, down to 1.3 m. In this study, measurements performed at a single point (close to the MUREX flux station) are used. Once properly calibrated, the neutron probe technique allows accurate measurements of the soil water content. The volumetric soil moisture measurements of 1995 are displayed in Fig. 3. Using the estimated soil moisture content change together with the measured precipitation and cumulated evaporation, it is possible to assess the water balance.

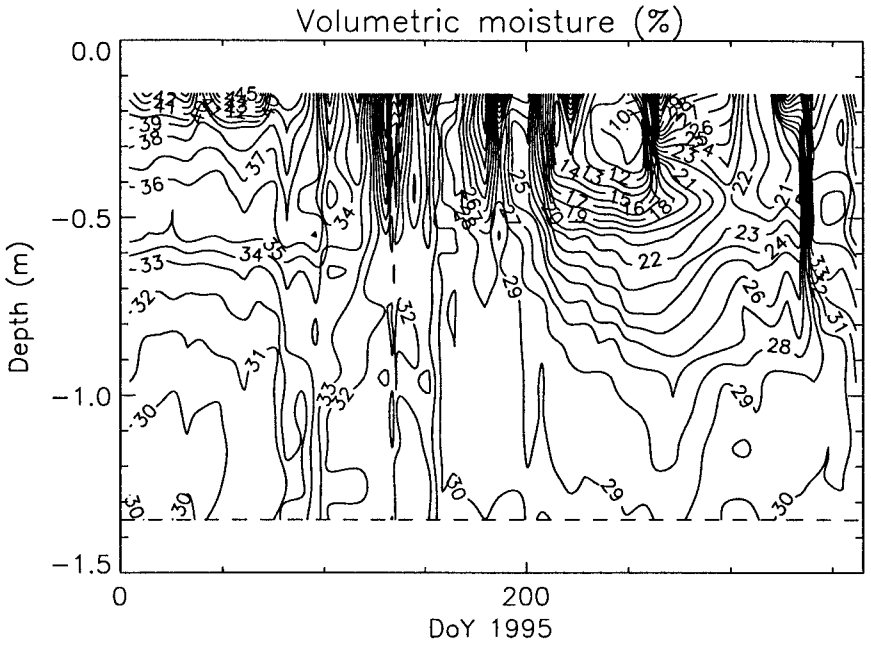

FIG. 3. Temporal diagram of the soil volumetric moisture within the surface 1.3-m layer as measured with a neutron probe over the MUREX fallow in 1995.

3) WATER BALANCE

According to the available measurements, the water balance of the MUREX fallow is rather unrepresentative of the climatic or large-scale evaporation over southwestern France. Indeed, the cumulated estimated evapotranspiration is about 800 mm for 1995, whereas the value of the cumulated precipitation for the same period is 770 mm. The evaporation excess can be explained by a local subsurface soil water convergence that is likely to occur in this kind of terrain. The in situ measurements of bulk soil moisture, precipitation, and evapotranspiration can be employed to estimate the weekly water excess Xs:

$$\mathrm{Xs} = \Delta\theta + \Sigma\,\mathrm{LE} - \Sigma\,P, \tag{2}$$

where $\Delta\theta$ is the change in the soil water content θ between two consecutive measurements, from the surface to a depth of 1.3 m, and Σ LE and $\Sigma\,P$ are the cumulated values of evapotranspiration and precipitation over the considered period, respectively. The values of Xs are presented in Fig. 4. January 1995 is a period of runoff displaying negative values of Xs that are not plotted in Fig. 4 due to the uncertainty on Σ LE during this period (many missing values). Ten inflow episodes (positive peak values of Xs) can be observed from the beginning of spring to the middle of the autumn. Their sum over 1995 represents a deep water gain of 180 mm. The inflow can be due to lateral movement of water and (to a lesser extent) to capillarity rises from deeper soil layers. It produces a significant contribution to the local water balance, especially during the drying period.

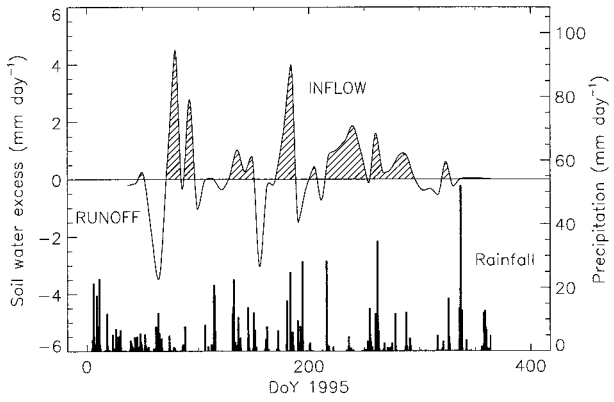

FIG. 4. The water excess (Xs) derived from the total soil moisture content, precipitation, and evapotranspiration measurements over the MUREX fallow in 1995. Positive values correspond to a net inflow from an upstream subsurface water table. Negative values indicate a net runoff. The measured precipitation is indicated.

The tensiometric measurements at the bottom of the profile show that upward head gradients occur only after 1 June 1995. The measured gradients of water potential between the 1.2- and 1.3-m layers can be used to assess the amount of water rising up from below after 1 June. Simple calculations based on typical values of saturation water content and hydraulic conductivity at saturation for the underlying clay bedrock indicate that the capillarity rises do not exceed 4 mm between 1 June and 31 December. Therefore, most of the water excess seems to be due to lateral movements of water. In the case of

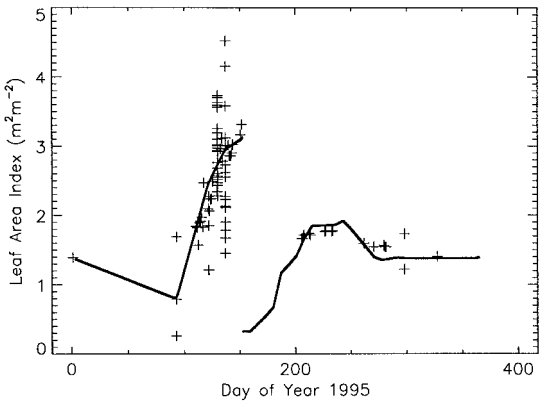

FIG. 5. The MUREX fallow green leaf area index in 1995 as measured (plus sign) and interpolated (solid line). The discontinuity on DoY 152 is due to the cutting of the vegetation.

the MUREX fallow, part of the inflow may be supplied by upstream rain and irrigation drained water (a large proportion of the uphill fields consists of irrigated maize). The effect of the local subsurface soil water convergence on the ISBA simulations and on retrieval of the bulk soil water content is discussed in sections 3b and 4.

b. Vegetation characteristics

The vegetation of the MUREX fallow consists of many herbaceous plant species whose growing cycles overlap, contributing to maintain a rather dense, evergreen canopy. The dead vegetation residues tend to form a rather dense vegetal mulch at the soil surface. In 1995, the fallow was mown on DoY 152, thus increasing the mulch dead biomass. During 1995, biweekly measurements of the canopy height were made. The maximum height of the canopy was 0.7 m, before the cutting of DoY 152. Green leaf area index (LAI) measurements were performed by destructive planimetric measurements. Also, solar radiation interception measurements following the same technique as described in Bégué et al. (1996) were used to derive values of LAI through the method by Roujean (1996). Figure 5 shows the measured values of LAI together with the prescribed evolution curve. The LAI curve is defined according to the observations and represents a smooth evolution of LAI to be prescribed in the model. The large scatter of LAI before the cutting is due to a rather large heterogeneity of the vegetation species distribution. After the cutting, the fitted LAI curve was extrapolated by using the canopy height measurements through the simple regression relationship

$$\mathrm{LAI} = 6.9h, \tag{3}$$

where LAI is expressed in $m^2\ m^{-2}$, and h is the canopy height in m, with $r^2 = 99\%$ and a standard error of 0.1 $m^2\ m^{-2}$.

Using the shortwave radiation measurements mentioned before, it was possible to determine the albedo (α) of the canopy: $\alpha = 0.20 \pm 0.04$.

c. Surface soil moisture measurements

Soil moisture profiles within the top 5-cm soil layer were measured twice a day during two 30-day intensive observing periods (IOPs) in spring and autumn 1995: 1) from DoY 114 to 143 for the spring IOP and 2) from DoY 269 to 298 for the autumn IOP. Each measurement consists of the gravimetric moisture of 36 (6 layers $\times$ 6 sites) soil samples, determined by a direct oven-drying method. The soil moisture content was measured 1) from the surface to the 5-cm depth with a resolution of 1 cm and 2) for the 0.5-cm surface layer. The volumetric moisture θ_v ($m^3\ m^{-3}$) is derived from the gravimetric measurements θ_m (kilogram of water per kilogram of dry soil) by

$$\theta_v = \frac{\rho_b}{\rho_w}\theta_m, \tag{4}$$

where ρ_b is the soil dry bulk density and ρ_w is the density of liquid water (kg m^{-3}). The value of ρ_b did not change significantly from one IOP to the other: the measured values over the surface 5-cm layer are 1452 ± 87 and 1450 ± 114 kg m^{-3} on DoY 123 and 286, respectively.

d. Surface temperature and emissivity

In this study, four temperature measurements were considered: the infrared temperature (T_{IR}) is obtained from an infrared radiometer, and the soil temperatures at 1, 3, and 50 cm below the soil surface (T_{-1}, T_{-3}, and T_{-50}, respectively) are measured with platinum-resistance thermometers. The surface temperature T_s was derived from T_{IR} and an effective emissivity ($\varepsilon_{\mathrm{eff}}$),

$$T_s = \left(\frac{T_{\mathrm{IR}}^4}{\varepsilon_{\mathrm{eff}}}\right)^{1/4}. \tag{5}$$

The value $\varepsilon_{\mathrm{eff}} = 0.977$ could be estimated from Eq. (5) by assuming that $T_s = T_{-1}$ when no vertical gradients of temperature were observed at the soil surface (i.e., $T_{-1} = T_{-3}$) after the sunset, between 2000 and 2100 LST.

The thermal emissivity of the surface ε_s is (like other vegetation characteristics such as LAI, h, α) a structure parameter of the ISBA scheme. The value of ε_s can be retrieved from T_s and the radiation measurements. Indeed, the measured upwelling thermal emission of the surface Rs can be written as

$$\mathrm{Rs} = \varepsilon_s \sigma T_s^4 + (1 - \varepsilon_s)\mathrm{Ra}. \tag{6}$$

The value $\varepsilon_s = 0.97$ minimizes the rms difference between the measured value of Rs and the value given by Eq. (6): the rms difference is 10.6 W m^{-2} and the mean bias is less than 2 W m^{-2} over 1995.

3. Model and calibration

The ISBA scheme was developed at Météo-France by Noilhan and Planton (1989) in order to describe the surface processes in weather forecast and climate models. In this study, the most recent version of ISBA, implemented within the Météo-France global climate model ARPEGE by Mahfouf et al. (1995) is employed.

a. The ISBA surface scheme

The ISBA scheme simulates the surface fluxes (LE, *H, G*) and predicts the evolution of the surface-state variables using the equations of the force-restore method of Deardorff (1977, 1978). Five variables (surface temperature T_s, mean surface temperature T_2, surface soil volumetric moisture w_g, total soil volumetric moisture w_2, and the canopy interception reservoir W_r) are obtained through the prognostic equations presented in the appendix. It must be noted that ISBA does not need a root distribution: w_2 is the volumetric soil moisture associated to a bulk layer of thickness d_2, including the root zone. The surface soil moisture w_g is computed to estimate the evaporation from the soil surface, whereas the transpired water is extracted from w_2. The surface water amount from w_g is included in w_2. When the soil water fluxes are decoupled from the atmosphere (this occurs at nighttime without precipitation), the value of w_g is driven by w_2 and is restored to an equilibrium value w_{geq} [depending mainly on w_2 and soil texture: see Fig. 2 in Noilhan and Planton (1989)]. In this study, the contribution of the water excess caused by a perched aquifer or by deep capillarity rises (measured positive values of Xs) is accounted for in the water budget Eq. (A4) (left term).

When used in stand-alone simulations, the ISBA model is driven by measurements of incoming radiation, precipitation, atmospheric pressure, air temperature and humidity, and wind speed at a reference level. Also, vegetation characteristics such as leaf area index and canopy height must be prescribed. These parameters may change with time. The model has prognostic equations for surface soil moisture, soil moisture in the root zone, and surface temperature, but initial values of these variables are required. Furthermore, estimates of the deep temperature [T_c in Eq. (A2)] are required to avoid severe drifts of the cumulated model heat flux in the soil. In this study, the prescribed deep temperature is taken as the measured temperature at 50 cm below the soil surface (T_{-50}).

In the same way, the time series of Xs may be prescribed in Eq. (A4) in order to obtain a good agreement between simulated and observed values of *both* surface evapotranspiration and root-zone soil moisture. In general, positive values of Xs do not occur in the root zone and this term can be omitted in Eq. (A4). However, Fig. 4 shows that the Xs term is very significant in the case of the MUREX fallow. The value of Xs is estimated using Eq. (2) as the residual of the soil water balance. Therefore, part of the Xs plotted in Fig. 4 may consist of measurement errors of soil moisture, surface fluxes, and precipitation. Since it is difficult to determine whether the positive values of Xs are due to lateral inflows or to measurement errors of soil moisture, evapotranspiration or precipitation, the ISBA simulations presented in this paper were performed twice: either using the estimated positive values of Xs in Eq. (A4) or assuming that this term is negligible.

The description of the surface fluxes Rn, *H*, and LE is detailed in Noilhan and Planton (1989). The main prescribed parameters of the surface involved in the flux calculation are the surface albedo and emissivity (α and ε_s, respectively), the momentum and thermal roughnesses (z_0 and z_{0h}, respectively), and the vegetation LAI and minimal stomatal resistance [r_{smin} (s m^{-1})]. This latter term depends on the plant species making up the canopy and in general must be calibrated. The surface albedo and emissivity are prescribed from measurements, and z_0 is derived from the vegetation height estimates (h) through $z_0 = 0.13h$.

b. Calibration of the model

Before performing simulations of the surface-state variables, the structure parameters of the surface scheme must be determined. Table 1 displays the ISBA structure parameters either obtained from the in situ measurements, derived from the soil texture (w_{wilt}, w_{sat}), or calibrated (w_{fc}, γ, ε_s, C_V, r_{smin}, z_0/z_{0h}). In this section, the procedure to obtain calibrated values is detailed. In order to assess the impact of the estimated water excess on the simulations, the calibration of ISBA was performed in two different configurations.

1) By fitting the model according to the measured atmospheric fluxes and including the water excess estimates (Xs) in Eq. (A4). In this case, we assume that the flux measurements are correct and therefore that the soil water excess is related to the surface water fluxes (evapotranspiration and precipitation) and to changes in soil moisture [Eq. (2)].
2) By prescribing Xs = 0 mm s^{-1} and calibrating the model by adjusting the simulated root-zone soil moisture according to the soil moisture observations (instead of adjusting the simulated atmospheric fluxes). In this case, the simulated evapotranspiration is lower than the measured values and a higher (tuned) value of r_{smin} is prescribed.

1) USING THE ESTIMATED WATER EXCESS

The tuned surface emissivity ε_s is the value ensuring the energy conservation between the measured upwelling and downwelling longwave fluxes and the surface temperature T_s derived from the infrared measurements (see section 2d).

TABLE 1. The ISBA scheme soil and vegetation structure parameters over the MUREX fallow. The values are either prescribed, measured, calculated from continuous functions of the texture, or calibrated.

Symbol	Definition	Value	Source
Soil parameters			
d_2	Soil root depth	1.3 m	Prescribed
CLAY	Clay fraction	28%	Measured
SAND	Sand fraction	14%	Measured
w_{wilt}	Wilting point	0.20 $m^3\ m^{-3}$	Continuous functions
w_{fc}	Field capacity	0.35 $m^3\ m^{-3}$	Calibrated
w_{sat}	Saturation	0.48 $m^3\ m^{-3}$	Continuous functions
γ	Deep heat transfer contribution	1	Calibrated
Vegetation parameters			
veg	Vegetation coverage	95%	Measured
α	Albedo	0.20	Measured
ϵ_s	Emissivity	0.97	Calibrated
C_V	Thermal coefficient	8.6×10^{-6} K m^{-2} J^{-1}	Calibrated
r_{smin}	Minimum stomatal resistance	47 s m^{-1} (100 s m^{-1})*	Calibrated
z_0/z_{oh}	Roughness length ratio	10 000	Calibrated

* Assuming a zero water excess.

The field capacity given by the soil texture continuous functions of ISBA is $w_{fc} = 0.28\ m^3\ m^{-3}$, with the observed sand and clay fractions (14% and 28%, respectively) corresponding to the 1.3-m surface layer. This value is not consistent with the very stable total soil moisture of 0.35 (or higher) observed from DoY 1 to 100. Indeed, prescribing $w_{fc} = 0.28$ results in rapidly taking out (by drainage) the exceeding water content to a value of w_2 of 0.28. This suggests that the true equivalent value of w_{fc} over the 1.3-m soil column is 0.35. Such a discrepancy cannot be explained by the heterogeneity of the soil texture profile since $w_{fc} = 0.35$ corresponds to CLAY = 50% in the continuous functions employed in ISBA: such a high value of CLAY is not observed in the studied soil column. This conclusion implies that the employed simple continuous function is not able to account for more complex factors acting on the field capacity, such as the biological activity and the organic matter content.

The thermal conductivity of the vegetated surface C_V cannot be estimated easily, especially in the case of the MUREX fallow canopy, comprising a mulch. Since the heat storage in the soil (i.e., the cumulated flux G) is conditioned by C_V, its value can be determined by minimizing the cost function,

$$E_G = \frac{1}{n_{obs}} \sum_{i=1}^{n_{obs}} \left(\sum_{1}^{i} G_{obs} - \sum_{1}^{i} G_{sim} \right)^2, \qquad (7)$$

where n_{obs} is the number of measured values of G (G_{obs}) and G_{sim} the corresponding simulated values, on a 30-min basis. The optimization was carried out using a quadratic interpolation method (PV WAVE 1993). The obtained optimal value of C_V (8.6×10^{-6} K m^2 J^{-1}) is significantly lower than the value employed in the ARPEGE climate simulations [2×10^{-5} K m^2 J^{-1}, Mahfouf et al. (1995)]. This low value of C_V can be related to the insulating effect of the mulch, with a relatively high heat storage.

The values of r_{smin} and z_0/z_{0h} were obtained by minimizing the cost function representing the error in the description of the fluxes at the surface–atmosphere interface:

$$E_F = \frac{1}{n_{Robs}} \sum_{1}^{n_{Robs}} (\mathrm{Rn}_{obs} - \mathrm{Rn}_{sim})^2 + \frac{1}{n_{Hobs}} \sum_{1}^{n_{Hobs}} (H_{obs} - H_{sim})^2 + \frac{1}{n_{Lobs}} \sum_{1}^{n_{Lobs}} (\mathrm{LE}_{obs} - \mathrm{LE}_{sim})^2, \qquad (8)$$

where n_{Robs}, n_{Hobs}, and n_{Lobs} are the number of measured values of Rn (Rn_{obs}), H (H_{obs}), and LE (LE_{obs}), respectively. The corresponding Rn_{sim}, H_{sim}, and LE_{sim} terms are the simulated values, on a 30-min basis. There are many ways to define the cost function, according to the available data and to the purpose of the optimization. In this study, the cost function E_F [Eq. (8)] represents the overall error in partitioning of energy at the surface–atmosphere interface. In order to take advantage of all the available data in the model calibration, Eq. (8) includes three terms corresponding to independent flux measurements (Rn, H, and G through the evapotranspiration value calculated by difference). It is verified that the minimized E_F function corresponds to a modeled water balance close to the observed one (rather low values of the rms error and mean bias over LE are indicated in Table 2).

The values of the simulated instantaneous and cumulated fluxes obtained with the structure parameters listed in Table 1 are compared with the observed values in Figs. 6 and 7, respectively. The errors affecting the simulated fluxes are listed in Table 2 in terms of rms error and mean bias (simulated minus observed). The rms error affecting the simulated G is 55 W m^{-2}. Such a large error may be explained by the influence of the

TABLE 2. Errors affecting the simulated flux densities with the calibrated model, in terms of rms error and mean bias (simulated minus observed) over evapotranspiration (LE), heat flux (*H*), net radiation (Rn) and soil heat flux (*G*).

Fluxes	LE	*H*	Rn	*G*
rms error (W m^{-2})	42	29	18	55
Mean bias (W m^{-2})	2	9	12	0

mulch: in reality, the heat storage in the soil is conditioned by the mulch, whereas the measured *G* was obtained from heat flux plates buried at a 3-cm depth in the soil. Therefore, the simulated *G* (at the mulch surface) displays a much larger diurnal cycle than the measured one (Fig. 6). On the other hand, the mean bias over *G* is very small (Table 2) and the cumulated flux is very well simulated (Fig. 7), especially before the cutting. The largest bias in Table 2 is associated with the simulated Rn and *H*. Also, the cumulated difference in Fig. 7 is rather large (about 100 mm) for both fluxes. The overestimation of Rn is consistent with the overestimation of *H* and suggests that the modeled surface temperature is underestimated (because more energy is removed from the surface through the heat flux in the model). Moreover, errors in *H* may be due to uncertainties in the estimation of z_0. The latent heat flux occupies an intermediate position: both the flux density and the cumulated flux are relatively well simulated. The high value of the observed cumulated evapotranspiration (Fig. 7) is well reproduced by the model with a rather low minimum stomatal resistance: $r_{smin} = 47$ s m^{-1}. It must be noted that this value is comparable with previous calibrations of ISBA over grasslands (Noilhan et al. 1992). The calibrated ratio z_0/z_{0h} reaches a high value of 10 000, whereas a value of 10 is usually employed for small vegetation canopies. However, many authors have reported high values of z_0/z_{0h} (even higher than 10 000) for a wide range of surfaces [see Verhoef et al. (1997) for a review; also Troufleau et al. (1997)]. Verhoef et al. (1997) suggest that $z_0/z_{0h} = 10$ is probably too low for most natural surfaces.

2) ASSUMING NO WATER EXCESS

In this second calibration, Xs = 0 mm s^{-1} in Eq. (A4). Since the amount of water supplied to the system is sharply reduced, the simulated evapotranspiration must also be lowered if the bulk soil water content is to be correctly reproduced. In this case, the cost function to be minimized in the calibration of ISBA is the rms difference between the simulated and measured time series of root-zone soil moisture. It was found that the

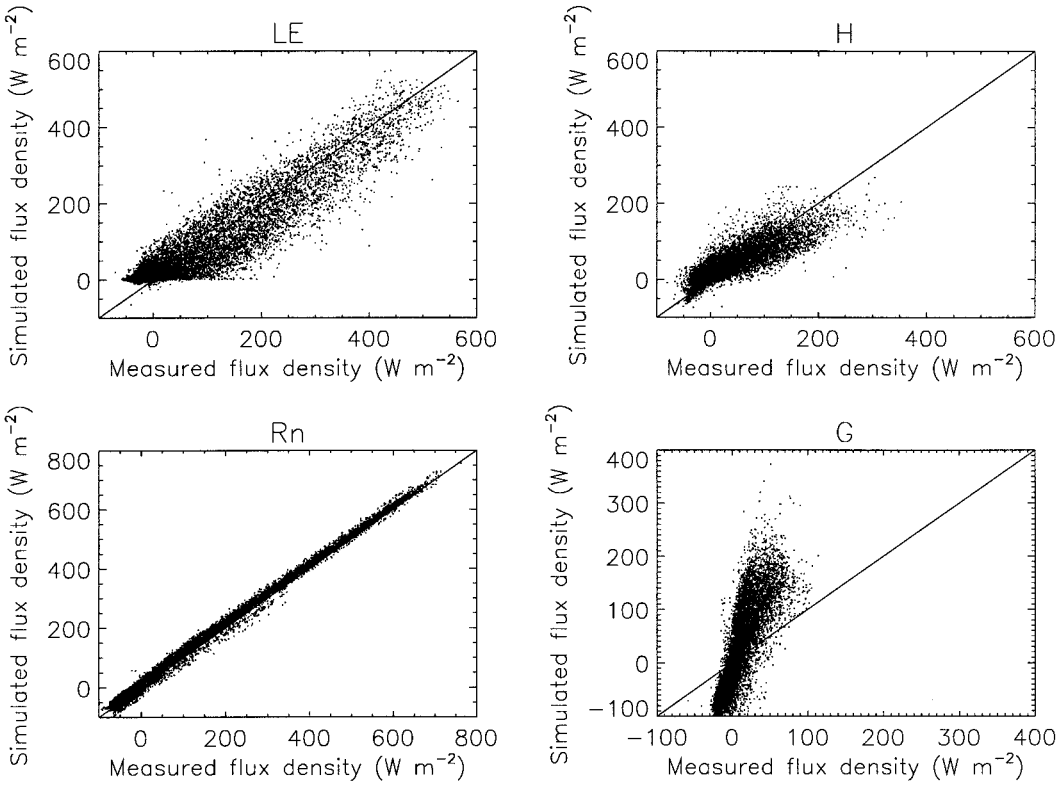

FIG. 6. Comparison between the simulated and measured fluxes of water vapor (LE), heat (*H*), net radiation (Rn), and heat storage in the soil and the biomass (*G*).

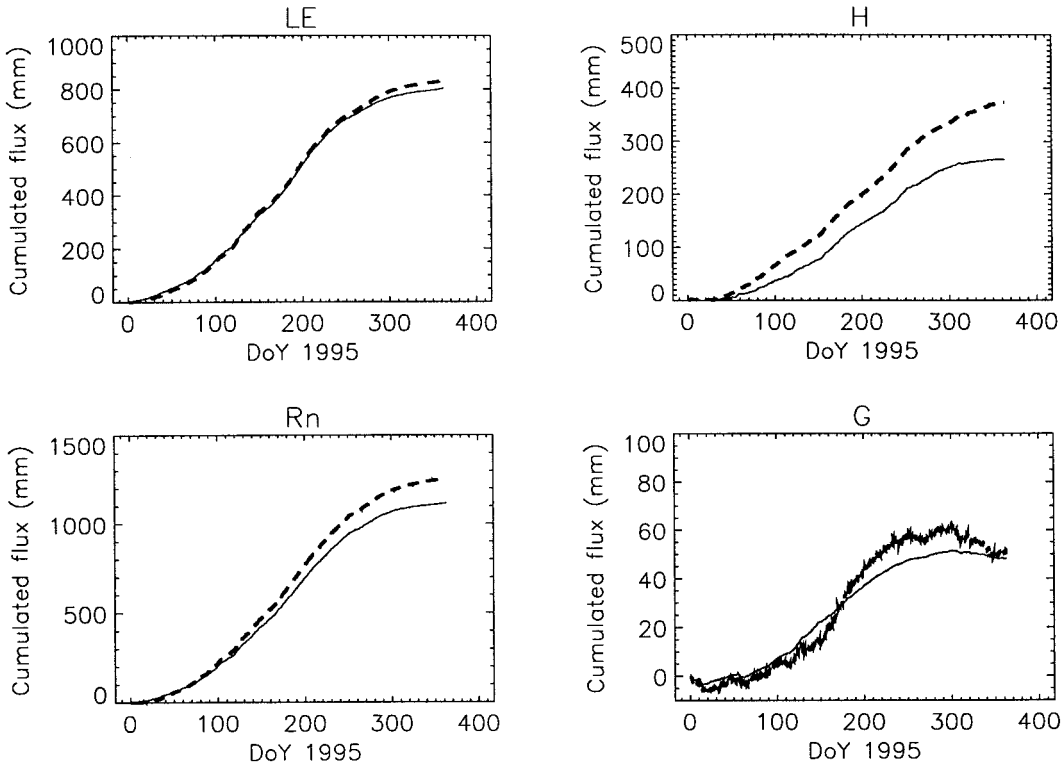

FIG. 7. As in Fig. 6 except for cumulated fluxes (mm). The solid and the thick dashed lines represent the measured and the simulated values, respectively.

optimum value of r_{smin} is 100 s m^{-1}: the soil water content $w_2 \times d_2$ (expressed in units of millimeters of an equivalent water layer) is simulated with an rms error of only 17 mm. A consequence of imposing Xs = 0 mm s^{-1} in Eq. (A4) is the discrepancy between the simulated and observed latent heat flux (Table 3). The mean bias is now -12 W m^{-2} over LE, against 2 W m^{-2} in the reference simulation (Table 2), and the cumulated simulated evapotranspiration is about 650 mm (instead of the measured 800 mm), a value in agreement with the climatology (Choisnel 1998). However, the different assumptions about the value of Xs have no repercussions on the root-zone soil moisture and field capacity retrievals presented in section 5.

TABLE 3. Errors affecting the simulated flux densities with the calibrated model assuming Xs = 0 mm s^{-1} in Eq. (A4). The rms error and mean bias (simulated minus observed) over evapotranspiration (LE), heat flux (*H*), net radiation (Rn), and soil heat flux (*G*) are indicated.

Fluxes	LE	*H*	Rn	*G*
rms error (W m^{-2})	56	32	17	61
Mean bias (W m^{-2})	-12	19	9	2

4. Simulation of the surface variables

Since the aim of this study is to investigate the link between w_2 and the surface prognostic variables T_s and w_g, it is important to verify that these variables are correctly reproduced by ISBA.

a. Simulation of the soil water contents

Figure 8 presents the simulated values of $w_2 \times d_2$ together with the observations in the case of the reference configuration (i.e., nonzero Xs and r_{smin} = 47 s m^{-1}). Like the zero-Xs simulation, the agreement is quite good, with an rms error of 16 mm. The two IOP dates are indicated in Fig. 8. The bulk soil water content is between 370 and 450 mm during the spring IOP and between 330 and 350 mm during the autumn IOP.

The comparison of w_g with the measured values is more complex since the ISBA surface soil moisture is not related to a prescribed depth of the surface layer. Since the measurements were performed at various depths (see section 2c), it was possible to calculate six values of the surface soil moisture corresponding to the soil layers between the surface and the 0.5-, 1-, 2-, 3-, 4-, and 5-cm depths. The mean bias and the square correlation coefficient r^2 between measured and simulated values were computed using a dataset comprising

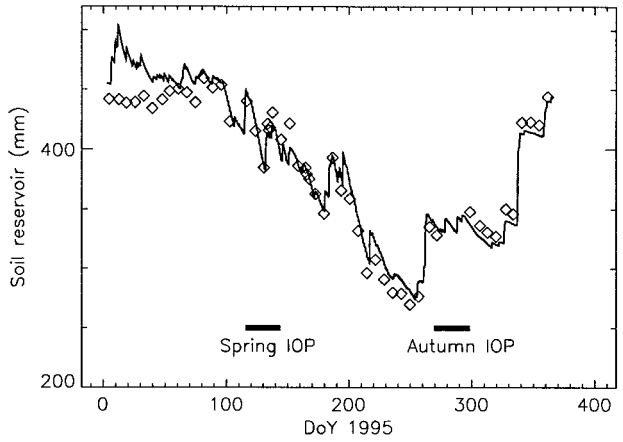

FIG. 8. The measured (diamonds) and simulated (solid line) soil water content of the 1.3-m soil column in 1995. The dates of the 30-day intensive observing periods (spring and autumn) are indicated.

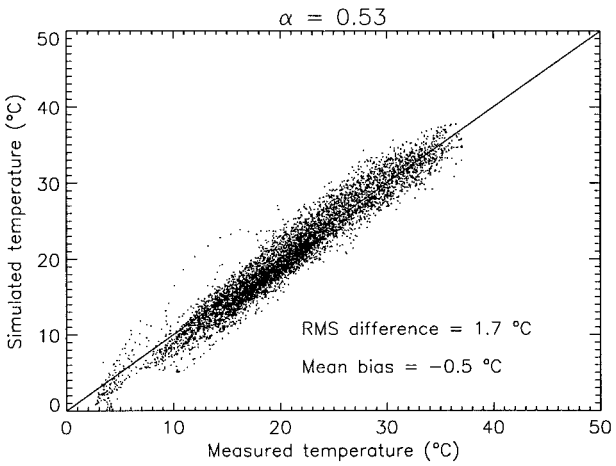

FIG. 10. The ISBA surface temperature vs the restored value of $T_i = \alpha T_s + (1 - \alpha)T_{-1}$ with $\alpha = 0.53$.

both spring and autumn IOP measurements. They are presented in Fig. 9 for the reference simulation. The best agreement is obtained for a depth of 5 cm, with r^2 higher than 75% and a negligible mean bias. The same result is obtained with the zero-Xs simulation.

b. Simulation of the surface temperature

On average, the simulated surface temperature tends to be lower than the measured T_s (mean bias of -2.1°C). This is consistent with the bias between the modeled and the observed Rn (Table 2). An explanation is that ISBA, being a single energy-budget model, tends to simulate a surface temperature that is representative of both vegetation and soil surface. Therefore, the surface temperature simulated by ISBA (T_i) can be approximated as an intermediate value between the infrared derived T_s and the soil temperature T_{-1}. An empirical mixing equation was employed to describe T_i:

$$T_i = \alpha T_s + (1 - \alpha)T_{-1}. \quad (9)$$

With $\alpha = 0.53$, the mean bias between the model surface temperature and the measured T_i is only -0.5°C, with a minimized rms error of 1.7°C for the reference simulation (Fig. 10). The zero-Xs surface temperature is closer to the infrared temperature, with $\alpha = 0.68$, a mean bias, and a minimized rms error of -0.3 and 1.8°C, respectively.

In this section, it was verified that ISBA is able to simulate the state variables of the surface with a reasonable accuracy. It was shown that the ISBA w_g is representative of the top 5-cm surface layer of the soil. The ISBA T_i represents a layer temperature described by the mixing of the infrared-derived top of the canopy and of the soil surface temperature. The question now to be adressed is whether w_2 is sufficiently related to w_g or T_i to be retrieved by inverting the ISBA scheme from estimates of w_g or T_i.

5. Inversion of the model

The results and figures presented in this section were obtained using the ISBA scheme in its reference con-

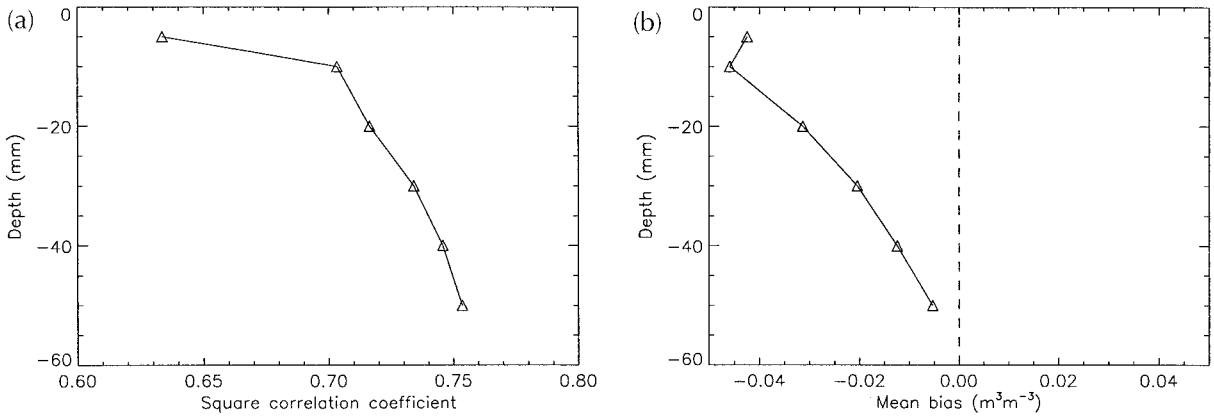

FIG. 9. Square correlation coefficient and mean bias between the simulated and measured surface soil moisture at 0.5, 1, 2, 3, 4, and 5 cm.

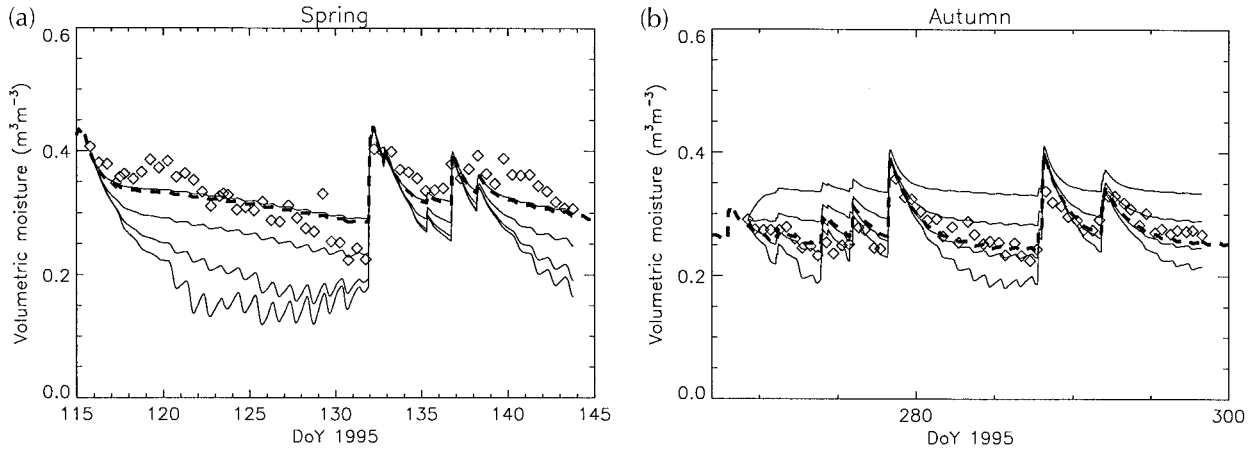

FIG. 11. The surface soil moisture w_g as measured over the top 5-cm soil layer (diamonds) and simulated by ISBA (thick dashed lines) during (a) the spring and (b) the autumn IOPs. The solid lines correspond to simulated w_g obtained with different values of w_2 imposed at the beginning of each IOP: 0.20, 0.25, 0.30, and 0.35 $m^3\ m^{-3}$. Higher prescibed values of w_2 impose higher values of the simulated w_g.

figuration (i.e., nonzero Xs and $r_{smin} = 47\ s\ m^{-1}$). Since the conclusions of the zero-Xs simulations are virtually the same, they are not presented here.

a. Total soil moisture content retrieval from the surface water content

In Fig. 11, the surface soil moisture w_g (as measured over the top 5-cm soil layer) is compared with the simulated values during the spring and autumn IOPs. The agreement is generally good. However, the measured w_g tends sometimes to remain longer above w_{fc} than predicted by ISBA or to decrease more rapidly, especially during the spring IOP. There are no obvious reasons to explain why the autumn comparisons are better than the spring ones. Given the simplicity of the description of the hydraulic phenomena at the surface by ISBA [Eq. (A3)], according to texture-dependent coefficients, such discrepancies are likely to occur. In particular, one factor may be the link between the soil hydraulic properties and the biological activity (e.g., galleries made by ants or worms): the soil structure (e.g., macroporosity) may change from one IOP to the other because of the biological activity. Since this factor is not accounted for in ISBA, the quality of the simulations may differ from one period to another. Another explanation is that the measurements of w_g seem less accurate during the spring IOP. For example, the increase of the spatially averaged measurements of w_g between DoY 117 and 120 (Fig. 11a) cannot be explained since no rain occurred during this period. Indeed, the standard deviation of the measured w_g is higher during the spring IOP: 0.033 $m^3\ m^{-3}$ versus 0.021 $m^3\ m^{-3}$ for the autumn IOP. The higher spatial variability of w_g during the spring IOP may be related to wet conditions, which prevailed during this period (the mean value of w_g is 0.34 $m^3\ m^{-3}$ versus 0.28 $m^3\ m^{-3}$ during the autumn IOP). The sampling strategy applied in this study (see section 2c) may be less efficient during the spring IOP because of the larger spatial variability. However, the overall agreement between observed and simulated values in Fig. 11 is acceptable.

Also, the sensitivity of the surface soil moisture to the total soil water content is shown in Fig. 11: the simulated w_g obtained with different values of w_2 imposed at the beginning of each IOP ($w_2 = 0.20$, 0.25, 0.30, and 0.35) differ a lot from one another. Different initial values of w_2 result in very distinct evolutions of the simulated w_g. This suggests that it is possible to obtain information about the total water content by observing the surface soil moisture. A priori, it is interesting to try to obtain information about the instantaneous value of w_2 and about the field capacity w_{fc}. Indeed, this latter variable corresponds to intrinsic properties of the soil, which cannot be easily determined from the texture (see section 3b).

1) RETRIEVING THE TOTAL SOIL MOISTURE CONTENT AT A GIVEN DATE

Assuming that the exact value of w_{fc} is known, the series of surface soil moisture measurements can be employed to estimate the total water content w_2. In this study, a simple assimilation technique was employed (Mahfouf 1991): a time series of w_g between the dates t and $t + T$ is employed to retrieve the initial value of w_2 (i.e., at the date t). The cost function to be minimized on time t is the rms difference between the measured and simulated values of w_g obtained between the dates t and $t + T$. Figure 12 presents the retrieved soil water content together with the cost function isolines for $T = 15$ days and $T = 5$ days. The cost function is displayed as a function of time t for values of w_2 ranging from 0.15 to 0.40 $m^3\ m^{-3}$. The employed method implies that the cost function cannot be calculated during the period T at the end of the considered IOP (hatched surfaces in Fig. 12) since measurements

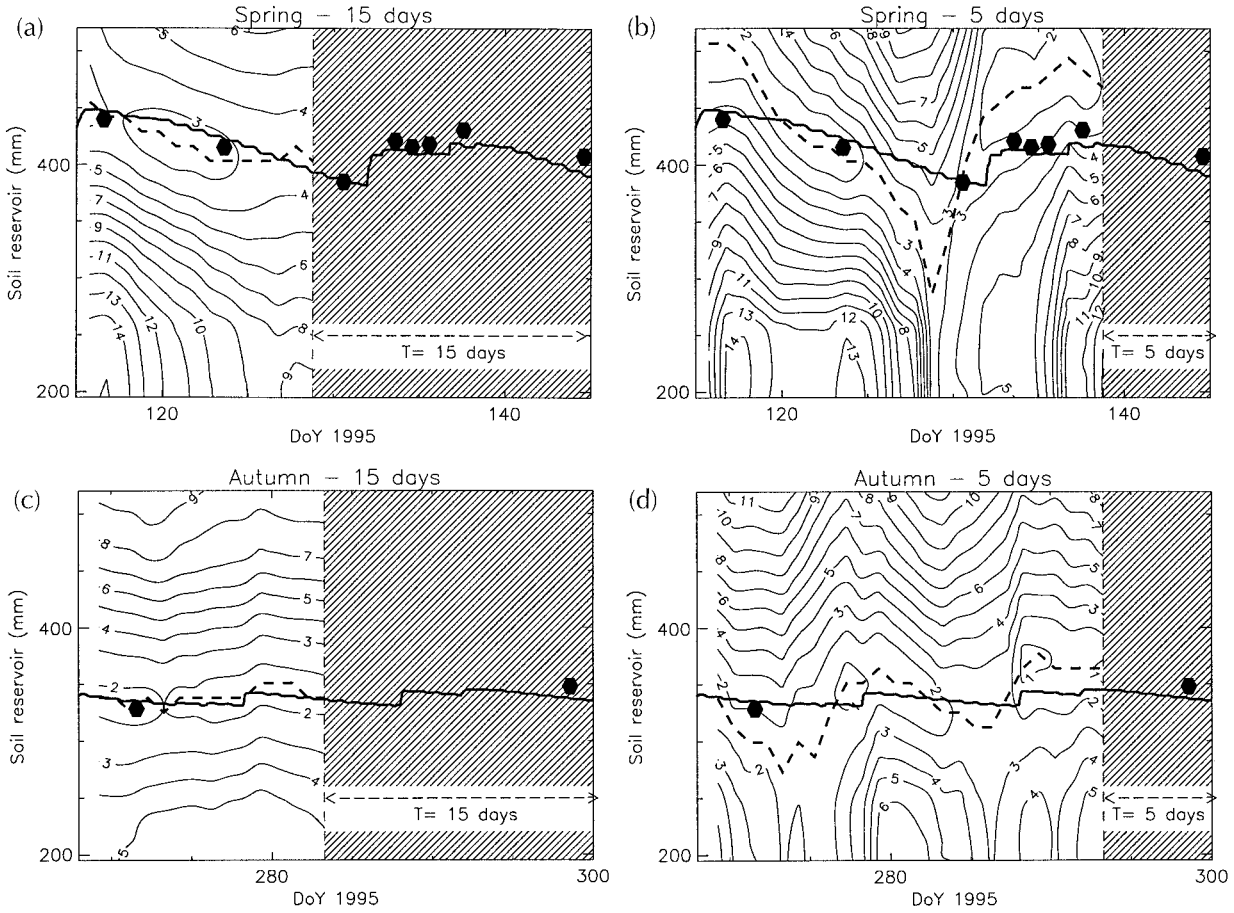

FIG. 12. Retrieved total soil water content (dashed thick line) compared with portions of the ISBA 1995 simulation (solid thick line) and the MUREX observations (dark points) also displayed in Fig. 8. (a) and (c): 15-day surface soil moisture series. (b) and (d): 5-day surface soil moisture series. (a) and (b): Spring IOP. (c) and (d): Autumn IOP. The solid isolines indicate the rms error (%) on the surface soil moisture over the period T (15 or 5 days) as a function of time and of the prescribed initial total soil moisture. The hatched surfaces correspond to the period T at the end of the considered IOP for which the rms error cannot be calculated.

would not be available on $t + T$. The retrieved w_2 corresponds to the minimum value of the cost function. It is very close to the measurements if a 15-day period is employed (Figs. 12a,c). On the other hand, large errors are observed with a 5-day period (Figs. 12b,d). This feature is related to the model errors concerning the hydraulic properties at the soil surface. The use of large time series ($T = 15$ days) tends to smooth out the errors and improve the accuracy of the retrieved soil water content. Several attempts have shown that time series less than 10 days should not be employed. Furthermore, employing a 15-day time series allows the reduction of the temporal resolution.

In Fig. 12, twice-daily measurements are employed. It can be shown that only a few observations of w_g are required to obtain the same precision as that of Fig. 12 for 15-day time series. Table 4 shows that including only one measurement of w_g every 3 or 4 days in the cost function is enough to obtain about the same accuracy. The obtained precision of the w_2 retrieval is excellent for the autumn IOP (rms error less than 14 mm) whatever the time lag between consecutive values of w_g (0.5–4 days). On the other hand, the rms error of the retrieved w_2 during the spring IOP increases with the time lag between consecutive values of w_g. This is related to the better ability of the model to simulate the measured surface soil moisture during the autumn IOP than during the spring IOP (see Fig. 11). The value of w_2 is correctly retrieved for time lags up to 3 days during the spring IOP (rms error less than 26 mm), but the error is too large beyond.

It must also be noted that since the diurnal cycle of w_g is nearly unnoticeable in the case of the MUREX fallow, the obtained result does not depend on the time of the measurement.

2) RETRIEVING THE FIELD CAPACITY

As shown in Fig. 8, the bulk soil water content remained at field capacity at the end of the winter. The spring IOP began on DoY 114, 1 day after heavy rains, ensuring field capacity conditions. Starting ISBA sim-

TABLE 4. Errors affecting the retrieved total soil water content w_2 using 15-day series of surface soil moisture (w_g) according to the time lag between two consecutive values of w_g for the spring and autumn IOPs. The rms difference and mean bias (retrieved minus reference) indicate the error between the retrieved w_2 (15 values, one per day) and the reference values (from the ISBA 1995 simulation, plotted in Fig. 12—solid thick lines).

Intensive observing period	Spring					Autumn				
Time lag between consecutive w_g (day)	0.5	1	2	3	4	0.5	1	2	3	4
Number of employed w_g	29	15	8	5	4	29	15	8	5	4
Maximum error (mm)	22.5	27.4	32.2	49.0	127.0	11.4	14.2	12.4	25.8	18.6
rms difference (mm)	12.9	15.2	18.5	26.0	42.2	6.5	9.1	6.1	13.4	11.0
Mean bias (mm)	−6.4	−11.0	−11.0	1.1	−7.3	2.7	2.7	1.5	7.0	3.4

ulations on DoY 114 assuming that the value of w_{fc} is equal to the initial prescribed w_2 (DoY 114) and comparing the obtained w_g with the measured ones as a function of this initial value of w_2 is a way to retrieve w_{fc}. Figure 13 presents the rms error of w_g (spring and autumn IOPs) as a function of the prescribed w_2 (DoY 114). The minimum error of w_g is observed for w_2 (DoY 114) = w_{fc} = 0.35, that is, for the real value of the field capacity. The best sensitivity is obtained during the spring IOP, which is closer to field capacity conditions. However, the autumn IOP data also provide information about w_{fc} since the correct value is indicated from these data in Fig. 13.

The proposed method is a combined fit of w_{fc} and the initial value of w_2. Since it relies on the assumption that the soil is at field capacity at the end of the winter season (which is often the case in temperate regions), this method should not be used after particularly dry years or in areas where the climatology does not allow the water recharge of the soil.

b. *Total soil moisture content retrieval from the surface temperature*

The surface temperature simulated by ISBA differs significantly from the infrared-derived one (Fig. 10).

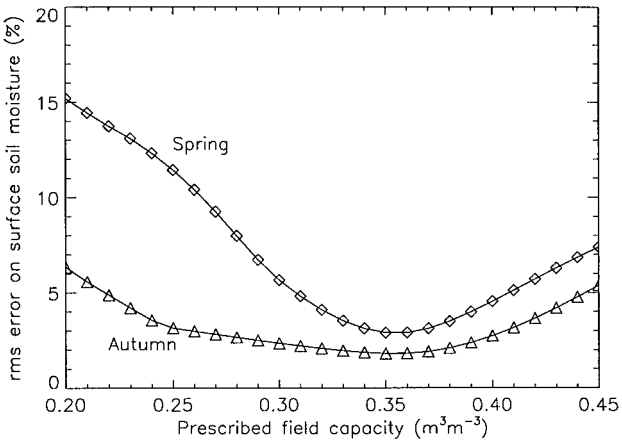

FIG. 13. Root-mean-square error on w_g (spring and autumn IOPs) as a function of the prescribed w_2 on DoY 114. It is assumed that, starting the ISBA simulations on DoY 114, the prescribed value of w_2 on DoY 114 is the value of w_{fc} during all the simulation period.

However, an attempt was made to retrieve the bulk soil water content from the hybrid temperature T_i [Eq. (9)] simulated by ISBA. In the case of the MUREX fallow, the link between the total water content and the surface temperature is controlled by the dense vegetation through the transpiration mechanism and the root system. Therefore, the sensitivity of the surface temperature to w_2 is expected to be at its most when the green transpiring leaves are well developed. More generally, all the factors favoring a high potential evaporation rate (such as high values of the solar radiation or high wind speeds) control this sensitivity (Wetzel et al. 1984). Therefore, the w_2 retrieval may be more or less difficult depending on the bioclimatic conditions. Again, it is investigated whether the observation of the surface variable over a given time period provides information about w_2.

The assimilation technique to retrieve the root-zone soil moisture from the surface temperature was applied to observations acquired between dates $t + T_0$ and $t + T_0 + T$ to retrieve the value of w_2 at the date t with $T = 2$ days and $T_0 = 3$ days. The ISBA simulations are started at time t using arbitrary initial values of the surface temperature and the surface soil moisture. The intermediate simulation period T_0 serves to obtain a value of the surface temperature and the surface soil moisture in equilibrium with the prescribed value of w_2. The w_2 retrieval was carried out using a quadratic interpolation method (PV WAVE 1993). The method was applied only for time periods displaying sufficient sensitivity of the simulated surface temperature to w_2. The criteria employed to ensure sufficient sensitivity (i.e., sorting cloudy periods, mainly) was

$$T_{i14}(w_2 = 0.20) - T_{i14}(w_2 = 0.35) \geq 5°\text{C}, \quad (10)$$

where T_{i14} is the surface temperature simulated by ISBA at 1400 LST.

The results are presented in Fig. 14. It appears that the w_2 retrieval is relatively successful only during a 50-day period (DoY 200–250). Apart from this period, the retrieved value is totally erroneous. Often, the optimization algorithm drifts to the imposed maximum value (0.40) of w_2. Another factor to explain this season-dependent sensitivity is the value of w_2 itself: Fig. 15

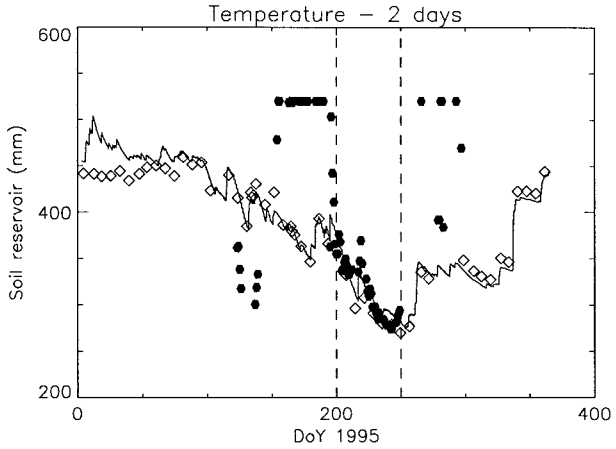

FIG. 14. Soil water content retrieval using 2-day series of surface temperatures from 1995. The retrieved values (dark points) are indicated together with the measured (diamonds) and simulated (solid line) soil water content of the 1.3-m soil column.

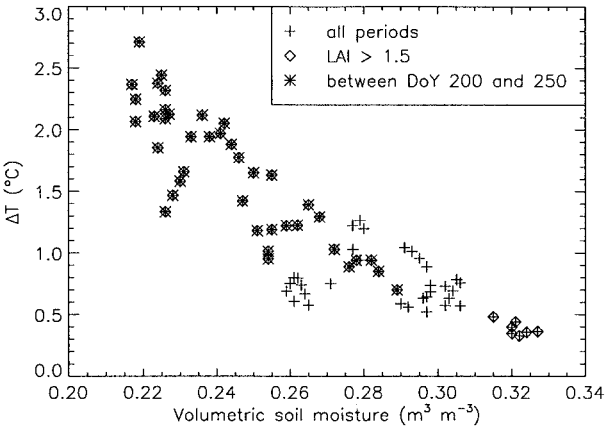

FIG. 15. Sensitivity (ΔT) of the simulated surface temperature vs the total soil moisture content w_2.

shows the sensitivity of the surface temperature to w_2. The sensitivity displayed in Fig. 15 (ΔT) is defined as

$$\Delta T = \frac{1}{n}\sum_{1}^{n}\left[T_i(w_2 - 0.025) - T_i(w_2 + 0.025)\right], \quad (11)$$

where $n = 96$ is the number of simulated values of the surface temperature in the 2-day period and w_2 is the observed value of the soil water content. It clearly appears that the highest values of ΔT are obtained in dry conditions. In particular, it is difficult to retrieve w_2 from surface temperature if $w_2 > 0.25$. In these wet conditions, the sensitivity (ΔT) is less than 1.7°C (i.e., less than the rms error on the simulated T_i).

This result confirms previous observations that the total soil moisture content is retrieved accurately from the surface temperature when the root zone is relatively dry (Wetzel et al. 1984; Taconet et al. 1986). In the case of a dense canopy, such a behavior is related to the employed parameterization of transpiration. For example, most of the surface schemes considered in the PILPS (Project for Intercomparison of Landsurface Parameterization Schemes) program (Chen et al. 1997), including ISBA, predict a rapid decrease of transpiration with soil moisture in relatively dry conditions above the wilting point (Mahfouf et al. 1996). On the other hand, transpiration varies little for wet soils close to the field capacity. It must also be noted that the formulations of transpiration are extremely variable between the models considered in PILPS and that ISBA is one of the models presenting the smoothest transition between stressed and unstressed conditions [see Fig. 2 in Mahfouf et al. (1996)]. Therefore, the conclusion that the use of surface temperature to retrieve the root-zone soil moisture is limited to rather dry conditions would certainly be confirmed by using other schemes.

6. Conclusions

The MUREX continuous micrometeorological and soil moisture observations of 1995 were employed to assess the ability of the simple surface scheme ISBA to properly simulate the energy and water budgets of a vegetated surface over a complete annual cycle. The surface scheme was modified to include the contribution of a local perched water table to the water balance. The surface soil moisture content measurements performed during two intensive observing periods show that ISBA is able to accurately reproduce this parameter, over a 5-cm-deep layer. On the other hand, the surface temperature simulated by the model is a combination of the surface temperature obtained by infrared radiometry and the temperature just below the soil surface.

Using the measurements of the surface soil moisture and the estimation of the ISBA hybrid temperature of the surface, it was possible to propose assimilation rules of these variables to retrieve the root-zone soil water content, knowing the atmospheric forcing and the precipitation. It was shown that four or five estimations of the surface soil moisture, at a low temporal resolution (one every 4 days, for example), are enough to retrieve the total soil water content by inverting ISBA. It was also shown that surface soil moisture series provide information about the field capacity of the soil. The use of the hybrid temperature is more problematic because its sensitivity to the value of the total water content is meaningful only in relatively dry conditions, over a well-developed canopy.

Primarily, the aim of MUREX is to provide continuous micrometeorological and soil moisture observations during several years in order to assess the ability of simple surface schemes employed in meteorology to properly simulate the energy and water budgets of the surface. Such a dataset could be useful to complete the ongoing intercomparison PILPS program (Chen et al. 1997). In particular, the PILPS program has shown that different parameterizations of soil water and runoff can

cause a very large variability in the simulated root-zone soil moisture. Also, the functional relationship between the parameterization of the root-zone soil moisture and the evapotranspiration vary from one model to another. This does not mean that the results obtained in this study are model specific. Any model designed to simulate the surface water balance and the root-zone soil moisture should succeed in retrieving the bulk soil moisture through the adequate assimilation technique based on surface observations. In this study, ISBA is able to simulate soil moisture remarkably well. In other situations, the ISBA scheme has proved to be reliable in terms of bulk soil moisture and evapotranspiration even over long time periods (e.g., Noilhan and Mahfouf 1996; Delire et al. 1998).

Finally, this study suggests that the use of passive microwaves in meteorology could help solve the problem of the soil water content estimation for two reasons: 1) many remote sensing studies have shown that it is possible to measure the surface soil moisture at L band (1.4 GHz) over a few centimeters' depth, even under rather dense canopies (Wang and Choudhury 1995; Wigneron 1995); 2) a surface temperature obtained by multifrequency microwave radiometry may be closer to the hybrid temperature simulated by a single energy budget model like ISBA than an infrared-derived one.

Further studies are needed to investigate the soil water content retrieval by simple surface schemes using estimations of the surface soil moisture and temperature provided by the analysis of passive microwave measurements (instead of employing direct or restored estimates). Also, the proposed assimilation technique must be tested under different conditions such as lower values of the soil water content or sparse vegetation.

Acknowledgments. This work was funded by the Conseil Régional de Midi-Pyrénées, the Programme de Recherche en Hydrologie (CNRS/INSU), and Météo-France/CNRM. The authors gratefully acknowledge the assistance of G. Lachaud, N. E. D. Fritz, G. Jaubert, P. Péris, F. Froissard, J.-L. Roujean at CNRM, C. Tosca at CESBIO (Toulouse), and J.-L. Thony at LTHE (Grenoble).

APPENDIX

Prognostic Equations

In the ISBA scheme, five variables (surface temperature T_s, mean surface temperature T_2, surface soil volumetric moisture w_g, deep soil volumetric moisture w_2, and the canopy interception reservoir W_r) are obtained through the following prognostic equations:

$$\frac{\partial T_s}{\partial t} = C_T(\mathrm{Rn} - H - \mathrm{LE}) - \frac{2\pi}{\tau}(T_s - T_2), \quad \text{(A1)}$$

$$\frac{\partial T_2}{\partial t} = \frac{1}{\tau}(T_s - T_2) - \frac{\gamma}{\tau}(T_2 - T_c), \quad \text{(A2)}$$

$$\frac{\partial w_g}{\partial t} = \frac{C_1}{\rho_w d_1}(P_g - E_g) - \frac{C_2}{\tau}(w_g - w_{g\mathrm{eq}}),$$
$$0 \le w_g \le w_{\mathrm{sat}} \quad \text{(A3)}$$

$$\frac{\partial w_2}{\partial t} = \frac{1}{\rho_w d_2}(P_g - E_g - E_{\mathrm{tr}} + \mathrm{Xs}) - \frac{C_3}{\tau}\max[0, (w_2 - w_{\mathrm{fc}})],$$
$$0 \le w_2 \le w_{\mathrm{sat}} \quad \text{and} \quad \mathrm{Xs} > 0, \quad \text{(A4)}$$

$$\frac{\partial W_r}{\partial t} = \mathrm{veg} \times P - E_r - R_r. \quad \text{(A5)}$$

The thermal conductivity term C_T in Eq. (A1) is expressed in units of K m^{-2} J^{-1} and represents the average conductivity of a patchy surface with a proportion, veg, covered by the vegetation (conductivity C_V) and 1-veg corresponding to bare soil (conductivity C_G):

$$C_T = \frac{1}{\left(\dfrac{1 - \mathrm{veg}}{C_G} + \dfrac{\mathrm{veg}}{C_V}\right)}. \quad \text{(A6)}$$

In Eqs. (A1)–(A4), τ is a restore time period of 1 day. The mean surface temperature T_2 is driven by the surface temperature T_s and the deep temperature T_c. Note that T_c must be prescribed, like the soil water excess term Xs [Eqs. (A2) and (A4), respectively]. In this study, $T_c = T_{-50}$, and the contribution of the deep heat transfers is represented by the γ coefficient. In Eqs. (A3)–(A5), the variables P and E correspond to precipitation and evaporation (or transpiration) rates, respectively. The subscripts g, tr, and r stand for ''ground level,'' ''transpiration,'' and ''intercepted water,'' respectively. In Eq. (A5), E_r represents the drainage from the interception reservoir W_r. The depth of the surface reservoir d_1 is an arbitrary normalization depth whose value does not change the predicted surface soil moisture w_g (expressed in units of m^3 m^{-3}). On the other hand, d_2 is the total soil reservoir depth and includes the root-zone soil layers related with the vegetation transpiration. The C_1, C_2, and C_3 coefficients describe the hydraulic properties of the soil affecting the infiltration at the surface, the subsurface conductivity, and the deep drainage or runoff (Mahfouf et al. 1995), respectively. The parameters w_{wilt}, w_{fc}, and w_{sat} are the values of the soil reservoir w_2 at wilting point (below which the plant transpiration stops), field capacity (maximum available water for transpiration), and saturation (maximum water content). The parameters w_{wilt}, w_{fc}, and w_{sat} depend on soil texture, and C_G, C_1, C_2, C_3, and $w_{g\mathrm{eq}}$ depend on

soil texture and soil moisture. They were expressed by Noilhan and Lacarrère (1995) and Mahfouf and Noilhan (1996) as continuous functions of the fraction of sand or clay (SAND and CLAY, respectively) in the root zone. Equation (A5) describes the evolution of the intercepted water reservoir (W_r) at the leaf surface.

REFERENCES

André, J.-C., J.-P. Goutorbe, and A. Perrier, 1986: HAPEX–MOBILHY: A hydrologic atmospheric experiment for the study of water budget and evaporation flux at the climatic scale. *Bull. Amer. Meteor. Soc.,* **67,** 138–144.

Bégué, A., J.-L. Roujean, N. P. Hanan, S. D. Prince, M. Thawley, A. Huete, and D. Tanré, 1996: Shortwave radiation budget of Sahelian vegetation. 1. Techniques of measurement and results during HAPEX–Sahel. *Agric. For. Meteor.,* **79,** 79–96.

Bessemoulin, P., and Coauthors, 1996: MUREX: Un programme de suivi du cycle annuel des échanges de masse et d'énergie entre sol, végétation, et atmosphère. Premiers enseignements. *Ateliers Expérimentation et Instrumentation,* Météo-France/CNRM, 289–294.

Calvet, J.-C., A. Chanzy, and J.-P. Wigneron, 1996: Surface temperature and soil moisture retrieval in the Sahel from airborne multifrequency microwave radiometry. *IEEE Trans. Geosci. Remote Sens.,* **34,** 588–600.

Chen, T. H., and Coauthors, 1997: Cabauw experimental results from the project for intercomparison of landsurface parameterization schemes (PILPS). *J. Climate,* **10,** 1194–1215.

Choisnel, E., 1998: Le cycle de l'eau dans le contexte français. *La Météorologie,* in press.

Deardorff, J. W., 1977: Parameterization of the ground-surface moisture content for use in atmospheric prediction models. *J. Appl. Meteor.,* **16,** 1182–1185.

——, 1978: Efficient prediction of ground temperature and moisture with inclusion of a layer of vegetation. *J. Geophys. Res.,* **83,** 1889–1903.

Delire, C., J.-C. Calvet, J. Noilhan, I. Wright, A. O. Manzi, and C. Nobre, 1998: Physical properties of Amazonian soils—A modeling study using the ABRACOS data. *J. Geophys. Res.,* in press.

Entekhabi, D., H. Nakamura, and E. Njoku, 1995: Retrieval of soil moisture profile by combined remote-sensing and modeling. *Passive Microwave Remote Sensing of Land–Atmosphere Interactions,* B. J. Choudhury, Y. H. Kerr, E. G. Njoku, and P. Pampaloni, Eds., VPS, 485–498.

Goutorbe, J.-P., 1991: A critical assessment of the Samer network accuracy. *Land Surface Evaporation. Measurement and Parameterization,* T. J. Schmugge and J.-C. Andre, Eds., Springer-Verlag, 171–182.

Mahfouf, J.-F., 1991: Analysis of soil moisture from near-surface parameters: A feasibility study. *J. Appl. Meteor.,* **30,** 1534–1547.

——, and J. Noilhan, 1996: Inclusion of gravitational drainage in a land surface scheme based on the force restore method. *J. Appl. Meteor.,* **35,** 987–992.

——, A. O. Manzi, J. Noilhan, H. Giordani, and M. Déqué, 1995: The land surface scheme ISBA within the Météo-France climate model ARPEGE. Part I: Implementation and preliminary results. *J. Climate,* **8,** 2039–2057.

——, and Coauthors, 1996: Analysis of transpiration results from the RICE and PILPS workshops. *Global Planet. Change,* **13,** 73–88.

McNider, R. T., A. J. Song, D. M. Casey, P. J. Wetzel, W. L. Crosson, and R. M. Rabin, 1994: Toward a dynamic-thermodynamic assimilation of satellite surface temperature in numerical atmospheric models. *Mon. Wea. Rev.,* **122,** 2784–2803.

Noilhan, J., and S. Planton, 1989: A simple parameterization of land surface processes for meteorological models. *Mon. Wea. Rev.,* **117,** 536–549.

——, and P. Lacarrère, 1995: GCM gridscale evaporation from mesoscale modeling. *J. Climate,* **8,** 206–223.

——, and J.-F. Mahfouf, 1996: The ISBA land surface parameterisation scheme. *Global Planet. Change,* **13,** 145–159.

——, J.-F. Mahfouf, A. Manzi, and S. Planton, 1992: Validation of land-surface parameterizations: Developments and experiments at the French weather service. *Proc. Validation of Models over Europe (2),* Reading, United Kingdom, ECMWF, 125–158.

PV-WAVE, 1993: Unconstrained minimization: Univariate and multivariate functions. *PV-WAVE Advantage Reference,* Visual Numerics, 231–250.

Roujean, J.-L., 1996: A tractable physical model of shortwave radiation interception by vegetative canopies. *J. Geophys. Res.,* **101**(D5), 9523–9532.

Schmugge, T. J., 1983: Remote sensing of soil moisture: Recent advances. *IEEE Trans. Geosci. Remote Sens.,* **GE-21**(3), 334–336.

Staley, D. O., and G. M. Jurica, 1972: Effective atmospheric emissivity under clear skies. *J. Appl. Meteor.,* **11,** 349–356.

Taconet, O., R. Bernard, and D. Vidal-Madjar, 1986: Evapotranspiration over an agricultural region using a surface flux/temperature model based on NOAA-AVHRR data. *J. Climate Appl. Meteor.,* **25,** 284–307.

Troufleau, D., J. P. Lhomme, B. Monteny, and A. Vidal, 1997: Sensible heat flux and radiometric surface temperature over sparse Sahelian vegetation. I. An experimental analysis of the kB^{-1} parameter. *J. Hydrol.,* **188–189,** 815–838.

van den Hurk, B., W. Bastiaanssen, H. Pelgrum, and E. van Meijgaard, 1997: A new methodology for assimilation of initial soil moisture fields in weather prediction models using METEOSAT and NOAA data. *J. Appl. Meteor.,* **36,** 1271–1283.

Verhoef, A., H. A. R. de Bruin, and B. J. J. M. van den Hurk, 1997: Some practical notes on the parameter kB^{-1} for sparse vegetation. *J. Appl. Meteor.,* **36,** 560–572.

Wang, J. R. and B. J. Choudhury, 1995: Passive microwave radiation from soil: Examples of emission models and observations. *Passive Microwave Remote Sensing of Land–Atmosphere Interactions,* B. J. Choudhury, Y. H. Kerr, E. G. Njoku, and P. Pampaloni, Eds., VSP, 423–460.

Wetzel, P. J., D. Atlas, and R. H. Woodward, 1984: Determining soil moisture from geosynchronous satellite infrared data: A feasibility study. *J. Climate Appl. Meteor.,* **23,** 375–391.

Wigneron, J.-P., 1995: Retrieval of geophysical parameters from multifrequency passive microwave measurements over a soybean canopy. *Passive Microwave Remote Sensing of Land–Atmosphere Interactions,* B. J. Choudhury, Y. H. Kerr, E. G. Njoku, and P. Pampaloni, Eds., VSP, 403–420.